



## Original Article

## Research on void drift between rod bundle subchannels

Shasha Liu<sup>a,b</sup>, Zaiyong Ma<sup>a,b,\*</sup>, Bo Pang<sup>c,\*\*</sup>, Rui Zhang<sup>a,b</sup>, Luteng Zhang<sup>a,b</sup>, Quanyao Ren<sup>d</sup>, Liangming Pan<sup>a,b</sup>

<sup>a</sup> Key Laboratory of Low-Grade Energy Utilization Technologies and Systems, Ministry of Education, Chongqing University, Chongqing, 400044, PR China

<sup>b</sup> Department of Nuclear Engineering and Nuclear Technology, Chongqing University, Chongqing, 400044, PR China

<sup>c</sup> Department of Nuclear Science and Technology, Shenzhen University, Shenzhen, 518060, PR China

<sup>d</sup> Science and Technology on Reactor System Design Technology Laborator, Chengdu, 610041, PR China



## ARTICLE INFO

## Keywords:

Rod bundle subchannels

Void drift

Void fraction

Flow regime

## ABSTRACT

Void drift between subchannels in a rod bundle is a crucial phenomenon affecting the calculation accuracy of thermal-hydraulic parameters in SMRs. It holds significant importance in enhancing the precision of safety analysis for SMRs. Existing research on experiment and model of void drift between rod bundle subchannels is relatively rare, and the accuracy of model calculations requires improvement. In this study, experiments on gas-liquid two-phase non-equilibrium flow were conducted to measure the redistribution of two-phase flow induced by void drift in a  $1 \times 2$  rod bundle. The experiment results indicated that in bubbly flow regime with void fraction less than 0.3, the void diffusion coefficient showed little variation with changes in void fraction. However, in slug flow and annular flow regimes with void fraction exceeding 0.3, the void diffusion coefficient significantly increased with an increase in void fraction. Furthermore, a new void drift model was developed and validated based on a subchannel code. The overall predicted uncertainty for the outlet void fraction in the rod bundle benchmark was less than 13%.

## 1. Introduction

A small modular reactor (SMR) such as small pressurized water reactors or small boiling water reactors, that is characterized by its reduced size, increased flexibility, and higher adaptability compared to traditional reactors [1–3]. SMRs such as ACPR50S, ACPR100S, ACP25S, and ACP100S have a similar rod bundle structure with traditional reactors, but higher safety is anticipated, so there is a requirement for development of refined models [4]. The subchannel model constitutes a classical approach for thermal-hydraulic safety analysis [5–7], positing that, in addition to axial main flow, there exist processes such as lateral transport, mixing, and exchange of momentum, mass, and energy between adjacent subchannels [8]. Among these processes, void drift occurs as a result of gas-liquid two-phase flow striving to reach an equilibrium state, causing bubbles to migrate between adjacent subchannels. This process is accompanied by the exchange of mass, momentum, and energy between subchannels.

In the past, various scholars have conducted experimental studies on

redistribution of void fraction caused by void drift [9–19] in rod bundle. Research indicated that void (either steam or gas) tended to migrate towards regions with relatively less flow resistance. Lahey et al. [10] observed that in Boiling Water Reactor (BWR), the flow quality in the central subchannels was much higher than in the corner and edge subchannels. This suggested the presence of a thick liquid film on the channel walls, while gas showing an apparent affinity for more open subchannels. In terms of modeling, Lahey and Moody [9–11] initially proposed a model called the "Void Settling Model". Later, Sadatomi [16] conducted experiments on void drift in two and multiple vertically aligned subchannels to improve the void drift model in subchannel analysis programs. The study also investigated the influence of channel arrangement and void fraction on void drift. It was concluded that the void drift phenomenon exhibits a subchannel size effect, with the void diffusion coefficient in triangularly arranged rod bundle channels being significantly smaller than in square arrangements. Kawahara et al. [20, 21], in experiments involving non-equilibrium two-phase flow of gas and water in triangularly arranged rod bundle channels, explored the

\* Corresponding author. Key Laboratory of Low-Grade Energy Utilization Technologies and Systems, Ministry of Education, Chongqing University, Chongqing, 400044, PR China.

\*\* Corresponding author.

E-mail addresses: [mazy@cqu.edu.cn](mailto:mazy@cqu.edu.cn) (Z. Ma), [bo.pang@szu.edu.cn](mailto:bo.pang@szu.edu.cn) (B. Pang).

<https://doi.org/10.1016/j.net.2024.03.033>

Received 9 November 2023; Received in revised form 18 February 2024; Accepted 21 March 2024

Available online 27 March 2024

1738-5733/© 2024 Korean Nuclear Society. Published by Elsevier B.V. This is an open access article under the CC BY-NC-ND license (<http://creativecommons.org/licenses/by-nc-nd/4.0/>).

impact of reducing surface tension on void drift. Based on a one-dimensional two-phase flow model, subchannel programs were used to predict flow and void redistribution. It was found that incorporating constitutive equations for wall friction and interface friction into the void drift model to account for the effect of reduced surface tension was effective for existing data.

Due to the complexity of the two-phase flow field in the subchannels and limitations in two-phase flow measurement techniques, there is a relative scarcity of research on void drift in experiments and models. Actually, in most subchannel analyses, the void diffusion coefficient is not carefully calculated, and in the void settling model, it is only roughly considered. Moreover, these models do not account for the influence of flow regimes. Considering these challenges, experiments were conducted on non-equilibrium gas-liquid two-phase flow to measure the redistribution of the gas-liquid flow caused by void drift between twin channels. Based on the obtained void diffusion coefficients, a novel new void drift model was developed. Also, The model was preliminarily validated based experimental results retrieved from rod bundle benchmark, offering support for enhancing the accuracy of thermal-hydraulic safety analyses in SMRs.

## 2. Experimental System

### 2.1. Experimental loop and test section

The experimental loop for void drift is illustrated in Fig. 1, comprising a water supply system, an air supply system, a test section, and a data acquisition system. An electromagnetic flowmeter is employed to measure the water flow rate, while a gas mass flowmeter is used to measure the air flow rate. Data acquisition is conducted through NI9220. The maximum uncertainty in flow rate measurement in the experiment is 3.20% for water, and 3.31% for air. To reduce the uncertainty of lateral mass flow generated by void drift, gas mass flowmeter 3 was calibrated using gas mass flowmeter 2 as a reference.

Several scholars have compared numerical simulations with experimental analysis and concluded that the flow field analysis results obtained from  $1 \times 2$  rod bundle subchannels computational model agree well with the experimental results in the central channel of a  $5 \times 5$  rod bundle [22–24]. To simplify the experiment, the test section adopted in this study is a dual-subchannel configuration. The cross-sectional structure, as shown in Fig. 2, has a pitch-to-diameter ratio of 1.326

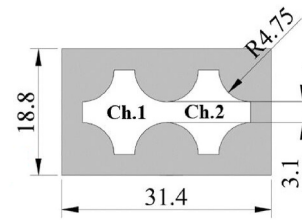


Fig. 2. Schematic diagram of cross-sectional structure of void drift section.

and a hydraulic diameter of 8.98 mm. The test section consists of an inlet section (axial height 1000 mm), a void drift section (axial height 70 mm), and an outlet section (axial height 930 mm). There are thin fins placed between the two subchannels in both inlet and outlet sections, and the void drift section has non-fins as depicted in Fig. 2. Pressure sensors are evenly distributed at the inlet and outlet of the void drift section to monitor the transverse pressure difference between the inlet and outlet.

### 2.2. Experimental procedure and operating conditions

The experimental process consists of the pre-experimental preparation and formal experimentation. The specific steps are described as follows :

Pre-experimental preparation.

- 1) Check the airtightness of the loop and ensure the pump is functioning properly.
- 2) Measure and record the conductivity and temperature of the water.
- 3) Measure and record the temperature of the air.

Formal Experimentation.

- 1) Open the water valve and air valve to fill subchannel 1 with water and subchannel 2 with a mixture of air and water.
- 2) Adjust the opening of the inlet water valve to achieve a 1:1 water flow rate ratio between the two subchannels.
- 3) Adjust the opening of the outlet valve and the frequency of the variable frequency pump to maintain a zero transverse pressure difference between the two subchannels at the entrance and exit of the test section (It should be noted, in reality, the difference of the transverse pressure difference was controlled to be less than 50 Pa). At the same time, ensure that the water and air flow rates reach the predetermined operating conditions.
- 4) Once the conditions are stable, record the flow rates of water and air at the inlet and outlet.
- 5) Repeat step 3, adjusting the water and air flow rates according to the operating conditions.

The experimental matrix consists of a total of 34 sets of operating conditions, with gas phase superficial velocity ( $j_g$ ) ranging from 0.10 to 3.00 m/s, liquid phase superficial velocity ( $j_l$ ) ranging from 0.35 to 1.00 m/s, and average void fraction ( $\alpha$ ) ranging from 0.04 to 0.5.

### 2.3. Void fraction measurement method

In this study, the drift flow model is used to calculate the void fraction, which is mainly calculated by the superficial velocity of gas phase and liquid phase obtained by experiment. Firstly, express the gas phase velocity as the sum of the mixture's superficial velocity and the local drift velocity of the gas phase. Therefore:

$$V_g = j + V_{gj} \quad (1)$$

Therefore, for the superficial velocity of the gas phase  $j_g$ :

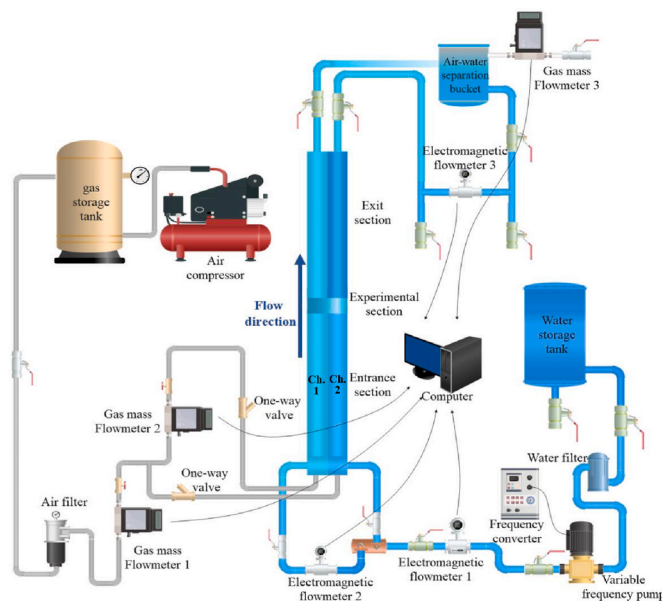


Fig. 1. Schematic diagram of the experimental system.

$$j_g = \alpha V_g = \alpha j + \alpha(V_g - j) \quad (2)$$

Taking the average of this equation across the cross-section, we obtain:

$$\{j_g\} = \{\alpha j\} + \{\alpha(V_g - j)\} \quad (3)$$

Note that the second term on the right-hand side is defined in terms of the drift velocity. Physically, it represents the rate at which the gas phase passes through a unit area (orthogonal to the channel's axial direction) with a velocity  $j$ . The superficial velocity of the gas phase can then be obtained from equation (3):

$$\{j_g\} = C_0 \{\alpha\} \{j\} + \{\alpha\} V_{gi} \quad (4)$$

The distributed parameter  $C_0$  in the equation is defined as:

$$C_0 \equiv \frac{\{\alpha j\}}{\{\alpha\} \{j\}} \quad (5)$$

The effective drift velocity is defined as:

$$V_{gi} \equiv \frac{\{\alpha(V_g - j)\}}{\{\alpha\}} \quad (6)$$

The void fraction  $\alpha$  can be obtained based on Equation (4):

$$\{\alpha\} = \frac{\{j_g\}}{C_0 \{j\} + V_{gi}} \quad (7)$$

### 3. Development of a new void drift model

According to the assumptions about void drift phenomenon by Lahey and Moody [9–11], void drift between subchannels in the rod bundle induces a convergence of the two-phase flow fields in the interacting subchannels towards an equilibrium state. As illustrated in Fig. 3, when there exists a disparity between the distribution of void fraction ( $\alpha_2 - \alpha_1$ ) in the interacting subchannels 1 and 2 and the distribution at equilibrium state ( $\alpha_2 - \alpha_1$ )<sub>EQ</sub>, void drift leads to an exchange between subchannels 1 and 2 through the gap. The mass flow rate of gas phase induced by void drift can be expressed as follows:

$$G_{VD} = \frac{(W_{2to1}^{VD})}{S_{12}} = \rho_g \tilde{D}_{VD} [(\alpha_2 - \alpha_1) - (\alpha_2 - \alpha_1)_{EQ}] \quad (8)$$

$$W_{2to1}^{VD} = (V_{20} - V_{21}) \rho_g A / L \quad (9)$$

$W_{2to1}^{VD}$  is the gas phase mass exchange flow rate per unit axial length induced by void drift,  $S_{12}$  is the gap between subchannels,  $G_{VD}$  is the gas phase mass exchange flow rate induced by void drift,  $\rho_g$  is the gas phase density.  $\tilde{D}_{VD}$  represents the void diffusion coefficient, characterizing the gas phase mass exchange rate between adjacent subchannels caused by void drift, similar to a gas phase diffusion coefficient induced by void drift.  $\alpha_1$  and  $\alpha_2$  represent the void fraction of the two interacting subchannels, respectively,  $(\alpha_2 - \alpha_1)$  is the difference in void fraction

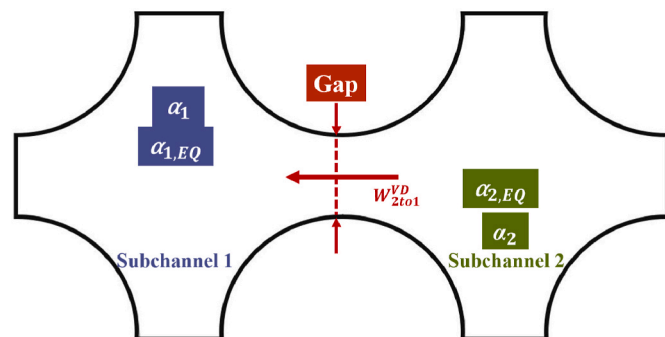


Fig. 3. Schematic representation of void drift phenomenon.

between the interacting subchannels in the current condition;  $(\alpha_2 - \alpha_1)_{EQ}$  is the distribution of void fraction in the two interacting subchannels under equilibrium conditions.  $V_{20}$  is the inlet gas phase superficial flow velocity for subchannel 2,  $V_{21}$  is the outlet gas phase superficial flow velocity for subchannel 2.

In this study, a fully symmetrical dual-subchannel configuration was employed. It can be assumed that under equilibrium condition, the void fraction in the two subchannels tends to be equal, meaning that  $(\alpha_2 - \alpha_1)_{EQ}$  tends towards zero. Therefore, under given operating conditions, the experimentally obtained  $G_{VD}$ ,  $\alpha_1$  and  $\alpha_2$ , combined with  $\rho_g$  and  $S_{12}$ , allow for the determination of the void diffusion coefficient  $\tilde{D}_{VD}$  for those conditions. A higher void diffusion coefficient  $\tilde{D}_{VD}$  indicates a more pronounced lateral exchange between adjacent subchannels due to the void drift phenomenon.

Among the conducted 34 operating conditions, the average void fraction of the  $1 \times 2$  rod bundle ranges from 0 to 0.55, covering typical flow regimes such as bubbly, slug, and annular flows. Typically, flow regimes are considered bubbly when the void fraction is less than 0.3, and slug or annular when it exceeds 0.3. Fig. 4 depicts the variation trend of the void diffusion coefficient  $\tilde{D}_{VD}$  with the average void fraction  $\alpha_{avg}$ . It can be observed that the inter-subchannel void drift is a lateral mixing phenomenon closely associated with the two-phase flow regimes.

Although the experimental data exhibits some scattering, it is still evident that in the bubbly flow regime with a void fraction below 0.3, the void diffusion coefficient shows little variation with changes in void fraction. However, in the slug and annular flow regimes with a void fraction exceeding 0.3, the void diffusion coefficient increases markedly with increasing void fraction. When the void fraction is raised from 0.3 to 0.5, the void diffusion coefficient increases by approximately an order of magnitude.

Based on the experiment data, empirical correlations for the void diffusion coefficient are separately fitted in a piecewise manner for the bubbly flow regime and the slug/annular flow regime. These correlations are functions of the average void fraction of interacting subchannels. Specifically, in the bubbly flow regime where the average void fraction is less than 0.3, the correlation is represented by the red fitted line in Fig. 4, which is given as:

$$\tilde{D}_{VD} = 5.593 \times \alpha_{avg} + 0.9265 \quad (10)$$

In contrast, in the slug and annular flow regimes where the average void fraction exceeds 0.3, the correlation is represented by the blue fitted line in Fig. 4, which is given as:

$$\ln(\tilde{D}_{VD}) = 9.6014 \times \alpha_{avg} - 1.966 \quad (11)$$

It should be noted, Equation (10) is applicable for void fraction ranging from 0.04 to 0.3, while Equation (11) is applicable for void fraction within the range of 0.3–0.5. Both empirical correlations are valid for a  $1 \times 2$  rod bundle configuration with  $P/d = 1.326$ ,  $d_e = 8.98$

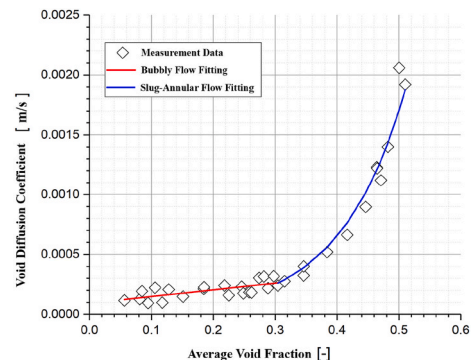


Fig. 4. Trend of void diffusion coefficient with average void fraction.

mm, and under operating conditions where the gas phase superficial velocity ( $j_g$ ) ranges from 0.10 to 3.00 m/s, and the liquid phase superficial velocity ( $j_l$ ) ranges from 0.35 to 1.00 m/s.

#### 4. Preliminary validation of the new void drift model based on rod bundle benchmark cases

This study employed a subchannel analysis code to perform validation calculations of the new void drift model, using experimental data provided by the rod bundle benchmark cases as a foundation.

##### 4.1. Preparation and compilation of data from rod bundle benchmark cases

The accuracy of the void drift model directly impacts the precision of subchannel analysis code in calculating local thermal-hydraulic parameters of rod bundle subchannels. Therefore, the local thermal-hydraulic parameters of rod bundle subchannels provided by measurements in the rod bundle benchmark cases are the foundation for validating the void drift model. In this study, the chosen benchmark cases are retrieved from the ISPRA rod bundle benchmark, which comprises two rod bundle test sections: the PELCO-S rod bundle test section simulating a typical boiling water reactor, and the EUROP rod bundle test section simulating a typical pressurized water reactor. For this research, only test cases obtained through the EUROP test section at typical PWR pressure levels (~160 bar) are selected for validating the void drift model.

The EUROP test section consists of a 4 × 4 square array of fuel rods, with an outer diameter of 10.75 mm and a rod-to-rod spacing of 14.3 mm (pitch-to-diameter ratio 1.330). The total axial length of the EUROP test section is 3660 mm, with seven supporting grids without mixing vane evenly spaced along the axial direction. In all the test conditions, both the axial and radial power distributions of the fuel rods are uniformly distributed.

Fig. 5 provides a cross-sectional schematic of the EUROP test section, where subchannels are categorized into six different types based on their specific positions within the bundle, represented by Arabic numerals in Fig. 5. Given the specified inlet average bundle mass flow rate, inlet bundle average temperature, and heating power, measurements were taken simultaneously at the outlet of five characteristic subchannels (as indicated in the shaded area in Fig. 4). At the outlet of these five characteristic subchannels, enthalpy and mass flow rate were measured, and the equilibrium gas void fraction of each subchannel was determined using the calorimetric method. To ensure steady-state conditions under predefined thermal-hydraulic boundary conditions and minimize measurement errors, sampling and measurement of subchannel outlet enthalpy and mass flow rate were carried out only after the entire experimental loop had been running continuously for several hours to achieve a stable state. According to the technical report of the ISPRA benchmark, the estimated maximum measurement error for subchannel mass flow rates and enthalpies is about 3%. Among the five sampled

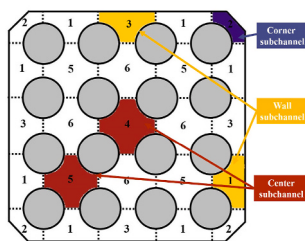


Fig. 5. Schematic Diagram of the Cross-Sectional Structure of the EUROP Rod Bundle Test Section Used in the ISPRA Benchmark Cases (The shaded area indicates five sampling subchannels utilized for flow rate and enthalpy measurements).

subchannels, there are three types: corner subchannel (labeled as #2), wall subchannels (labeled as #1 and #3), and center subchannels (labeled as #4 and #5).

##### 4.2. Implementation and initial validation calculations of the new void drift model

This study selected approximately 130 two-phase flow conditions with consistent outlet pressure (~160 bar), average bundle mass flow rate ranging from 2500 to 3500 kg/m<sup>2</sup>s, average inlet void fraction between -0.40 and -0.26, and average outlet void fraction between -0.05 and 0.20. These conditions were employed for the initial validation using the EVVD void drift model within the subchannel analysis code. Table 1 summarizes the key constitutive models within the subchannel code used for validation calculations, including pressure drop models, void fraction correlations, and lateral inter-subchannel mixing models. The void drift model selected void diffusion coefficients developed in this study that were applicable to different flow regimes.

The experimental measurement data for the rod bundle benchmark cases includes the subchannel outlet mass flow rate and the relative enthalpy rise in the subchannel. Table 2 summarizes the average ratio ( $P/M_{avg}$ ) of predicted values (P) to measured values (M) for different types of subchannels (including corner, wall, and center subchannels). It is observed that with the implementation of the new void drift model, the uncertainty in the subchannel analysis code’s calculation of local thermal-hydraulic parameters for subchannels is less than 13%.

## 5. Conclusion

This study conducted experiment and model study on void drift between rod bundle subchannels, leading to the following conclusions.

- (1) In the bubbly flow regime with a void fraction below 0.3, the void diffusion coefficient showed little variation with changes in void fraction. However, in the slug and annular flow regimes with a void fraction exceeding 0.3, the void diffusion coefficient increased markedly with increasing void fraction. When the void

Table 1  
Key constitutive models used for validation calculations.

Pressure	Single-Phase Turbulent Friction Coefficient	$0.184 \cdot Re^{-0.2}$
Drop	Two-Phase Friction Multiplier	Armand Model [25]
Model	Support Grid Pressure Drop Coefficient	0.944
Void	Subcooled Boiling Void Fraction	Levy Model [26]
Fraction Correlation	Saturated Boiling Void Fraction	Corrected Armand Model [27]
Lateral Inter-Subchannel Mixing Model	Cross-Flow Resistance Coefficient	0.5
	Single-Phase Turbulent Mixing Coefficient	0.005
	Two-Phase Turbulent Mixing Multiplier	Beus Model [28]
	Void Drift Model	$\tilde{D}_{VD} = 5.593 \times \alpha_{avg} + 0.9256 (0.04 < \alpha < 0.3)$ $\ln(\tilde{D}_{VD}) = 9.6014 \times \alpha_{avg} - 1.966 (0.3 < \alpha < 0.5)$

**Table 2**  
Accuracy of the new void drift model in predicting rod bundle outlet parameters.

	Corner Subchannel		Wall Subchannel		Center Subchannel	
	Relative Enthalpy Rise	Outlet Mass Flow Rate	Relative Enthalpy Rise	Outlet Mass Flow Rate	Relative Enthalpy Rise	Outlet Mass Flow Rate
$P/M_{avg}$	0.878	0.923	0.981	0.969	1.086	1.018

fraction was raised from 0.3 to 0.5, the void diffusion coefficient increased by approximately an order of magnitude.

- (2) Utilizing the existing subchannel code, combined with literature and experimental data, an improved void drift model was developed and validated. The overall predicted uncertainty for the outlet void fraction in the rod bundle benchmark was less than 13%.

#### Declaration of competing interest

The authors declared that they have no conflicts of interest to the enclosed manuscript entitled “Research on Void Drift between Rod Bundle Subchannels”. We declare that we do not have any commercial or associative interest that represents a conflict of interest in connection with the work submitted.

#### Acknowledgements

The authors appreciate the National Natural Science Foundation of China (U21B2059,12105273)

#### References

- [1] Guo Chengzhan, Haige Zhao, Progress of operation and application on Shenzhen MNSR, Chinese Journal of Nuclear Science and Engineering 20 (2000).
- [2] Huai-kun Jiang, et al., Application of MNSR epithermal neutron activation analysis in determination of geological sample, Atomic Energy Sci. Technol. 49 (8) (2015) 1488.
- [3] Li Yiguo, et al., Physics experimental study for reactor of in-hospital neutron irradiator, Atomic Energy Sci. Technol. 43 (2009).
- [4] M.D. Carelli, D.T. Ingersoll, Handbook of Small Modular Nuclear Reactors, 2014.
- [5] Chenglong Wang, et al., Sub-channel analysis for Pb-Bi-cooled direct contact boiling water fast reactor, Int. J. Energy Res. 42 (8) (2018) 2643–2654.
- [6] Hang Xia, et al., Development of a thermo-mechanical coupling code based on an annular fuel sub-channel code, Nucl. Eng. Des. 355 (2019) 110284.
- [7] Yonghong Tian, et al., Sub-Channel analysis of Pb-Bi-cooled reactor with modified COBRA-EN, in: International Conference on Nuclear Engineering, 45912, American Society of Mechanical Engineers, 2014.
- [8] J.T. Rogers, N.E. Todreas, Coolant Interchannel Mixing in Reactor Fuel Rod Bundles, 1969.
- [9] R.T. Lahey Jr., F.J. Moody, The Thermal-Hydraulics of a Boiling Water Nuclear Reactor, second ed., 1993.
- [10] R.T. Lahey, F.A. Schraub, Mixing, Flow Regimes, and Void Fraction for Two-phase Flow in Rod Bundles, 1969.
- [11] R.T. Lahey, et al., Out-of-pile subchannel measurements in a nine-rod bundle for water at 1000 psia, in: Proceedings of the International Symposium on Two-phase Systems 6, 1972, pp. 345–363.
- [12] José M. Gonzalez-Santaló, Two Phase Flow Mixing in Rod Bundle Subchannels, Diss. Massachusetts Institute of Technology, 1971.
- [13] Jr Lahey, T. Richard, Subchannel measurements of the equilibrium quality and mass flux distribution in a rod bundle, in: International Heat Transfer Conference Digital Library, Begel House Inc., 1986.
- [14] Y. Sato, M. Sadatomi, H. Tsukashima, Two-phase flow characteristics in interconnected subchannels with different cross-sectional areas, in: Proc. 1987 ASME• JSME Therm. Eng. Joint Cont., Honolulu 5, 1987, pp. 389–395.
- [15] A. Tapucu, et al., Experimental investigation of mass exchanges between two laterally interconnected two-phase flows, Nucl. Eng. Des. 105 (3) (1988) 295–312.
- [16] Sarman Gençay, Alberto Teyssedou, Peter Tye, Lateral mixing mechanisms in vertical and horizontal interconnected subchannel two-phase flows, Nucl. Technol. 138 (2) (2002) 140–161.
- [17] Michio Sadatomi, Akimaro Kawahara, Yoshifusa Sato, Flow redistribution due to void drift in two-phase flow in a multiple channel consisting of two subchannels, Nucl. Eng. Des. 148 (2–3) (1994) 463–474.
- [18] Michio Sadatomi, et al., Two-phase void drift phenomena in a 2× 3 rod bundle: flow redistribution data and their analysis, Nucl. Technol. 152 (1) (2005) 23–37.
- [19] M.P. Sharma, A.K. Nayak, Experimental investigation of void drift in simulated subchannels of a natural-circulation pressure tube-type BWR, Nuclear Science & Engineering the Journal of the American Nuclear Society (2017) 1–12.
- [20] A. Kawahara, M. Sadatomi, K. Kano, et al., Void diffusion coefficient in two-phase void drift for several channels of two-and multi-subchannel systems, Multiphas. Sci. Technol. 18 (1) (2006).
- [21] Akimaro Kawahara, et al., Void diffusion coefficient in two-phase void drift for several channels of two-and multi-subchannel systems, Multiphas. Sci. Technol. 18 (2006) 1.
- [22] Ulrich Bieder, François Falk, Gauthier Fauchet, LES analysis of the flow in a simplified PWR assembly with mixing grid, Prog. Nucl. Energy 75 (2014) 15–24.
- [23] I.I.L.D. Smith, et al., Benchmarking computational fluid dynamics for application to PWR fuel, in: International Conference on Nuclear Engineering, 35979, 2002.
- [24] Moysés A. Navarro, AC Santos André, Evaluation of a numeric procedure for flow simulation of a 5× 5 PWR rod bundle with a mixing vane spacer, Prog. Nucl. Energy 53 (8) (2011) 1190–1196.
- [25] Aleksandr Aleksandrovich Armand, The resistance during the movement of a two-phase system in horizontal pipes, Izv. Vses. Teplotekh. Inst. 1 (1946) 16–23.
- [26] Salomon Levy, Forced convection subcooled boiling—prediction of vapor volumetric fraction, Int. J. Heat Mass Tran. 10 (7) (1967) 951–965.
- [27] K.H. Sun, R.B. Duffey, C.M. Peng, The prediction of two-phase mixture level and hydrodynamically-controlled dryout under low flow conditions, Int. J. Multiphas. Flow 7 (5) (1981) 521–543.
- [28] S.G. Beus, Two-phase Turbulent Mixing Model for Flow in Rod Bundles, No. WAPD-T-2438; CONF-711112-6, Bettis Atomic Power Lab., Pittsburgh, Pa, 1972.